Results in Engineering 25 (2025) 104350

Contents lists available at ScienceDirect

Results in Engineering

journal homepage: www.sciencedirect.com/journal/results-in-engineering

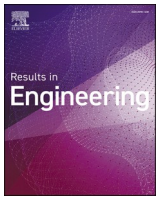

Research paper

Maghnite grafting with (3-Mercaptopropyl) triethoxysilane and its influence on the interlamellar distance blocking value

Deghfel Nadir [a,*], Melouki Azzedine [b], Benyahia Azzedine [a], Farsi Chouki [c], Laib Nouri [b], Khodja Mohammed Abdallah [b]

[a] City, Environment, Hydraulics and Sustainable Development Laboratory, Department of Chemistry, Faculty of Sciences, University of M'sila, University Pole, Road Bordj Bou Arreridj, M'sila 28000 Algeria
[b] Inorganic Materials Laboratory, Department of Chemistry, Faculty of Sciences, University Pole, Road Bordj Bou Arreridj, M'sila 28000 Algeria
[c] Materials and Mechanical Structure Laboratory (LMMS), Department of Mechanical Engineering, Faculty of Sciences and Technology, University Pole, Road Bordj Bou Arreridj, M'sila 28000 Algeria

ARTICLE INFO

Keywords:
Montmorillonite
Grafting
Silane
Basal distance
Intercalation
Surfactant
Cation exchange capacities

ABSTRACT

Maghnite (Algerian Montmorillonite) was grafted with (3-Mercaptopropyl)triethoxysilane in a water/ethanol mixture. The intercalation phenomenon of the grafted product was investigated following a modification with trimethyltetradecylammonium chloride at different cation exchange capacities (CEC). XRD results revealed a fixation of the d_{001} value at 21.47 Å after the grafting reaction, caused by the condensation of silane molecules with the two adjacent clay layers. This effect was not observed during the modification of non-grafted montmorillonite with the same surfactant, as the d001 value increased with higher concentrations of trimethyltetradecylammonium chloride. TGA analysis revealed the hydrophobic nature of the modified material, initially hydrophilic, with a reduction in the loss of physisorbed and chemisorbed water from 11.36 % to 6.73 %, thus limiting the swelling phenomenon. The absorption bands at 2954.4 cm^{-1}, 2854.4 cm^{-1}, and 2569 cm^{-1}, assigned to -CH_2 (symmetric), -CH_2 (asymmetric), and SH groups, respectively, confirm the successful grafting and intercalation. Controlling the fixation of the interlayer spacing of a clay grafted with an alkoxysilane can lead to the development of an organophilic material with immobilized reactive organic groups and controlled swelling.

1. Introduction

The synthesis of organophilic clays (hybrid materials or nanocomposites) that can be used, for example, as catalytic supports in reactions for the conversion of certain organic compounds as environmental materials or as auxiliaries in the synthesis of solar panels [1–3] has attracted the interest of many researchers. Silane grafting has proven to be an effective method for changing the appearance of clay surfaces. Several studies on the functionalization of clays have been conducted in order to synthesize organic-inorganic hybrid materials in which the two parties are linked by strong interactions (covalent bonds), favoring a certain immobilization of reactive organic groups on clay surfaces and preventing their leaching into the surrounding environment when used in solutions [4,5].

Among these clays is montmorillonite, widely used to prepare this material [6,7]. Montmorillonite clay is a typical aluminosilicate representative. It possesses several unique properties, including a lamellar structure, swelling capacity, special hydration capacity, adsorption, and interlayer ion exchange capacity. This last property qualifies montmorillonite for possible modification by precursors (silanes). This mineral has an excess negative charge on its surface, which allows cations to be easily absorbed [8,9]. This surface charge can thus be neutralized by modifying the surface with cationic organic surfactants [10,11]. Montmorillonite is a hydrophilic mineral that can only interact with polar structures. Thus, mixing this type of mineral with apolar hydrophobic compounds would be extremely difficult. Hydrophobic groups must be introduced to the surface of the layers to overcome this barrier and enable organo-mineral interactions [12]. Previous research has shown that introducing organic complexes between montmorillonite layers changes the surface's hydrophilic properties, making it hydrophobic [13]. This modification method may be possible by reacting silanes with silanol groups (Si-OH) located on this type of clay sheet's edges and surfaces [14–16]. A previous study found that the silane was inserted into the interfoliar space of montmorillonite due to an increase in basal

* Corresponding author.
E-mail address: nadir.deghfel@univ-msila.dz (D. Nadir).

https://doi.org/10.1016/j.rineng.2025.104350
Received 13 December 2024; Received in revised form 29 January 2025; Accepted 11 February 2025
Available online 15 February 2025

spacing (d_{001}), with the high value of the latter explained only by the presence of a double layer of silane molecules connecting the two adjacent layers of montmorillonite [17]. The technique involves exposing these silanols to organosilane agents [18].

Several studies have shown that grafting a silane onto montmorillonite, such as aminopropyltrimethoxysilane, increased its d_{001}, confirming the possibility of grafting into the galleries of montmorillonite

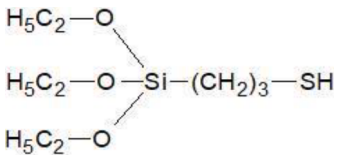

Eqs. (1) and (2) express the hydrolysis and grafting reactions:

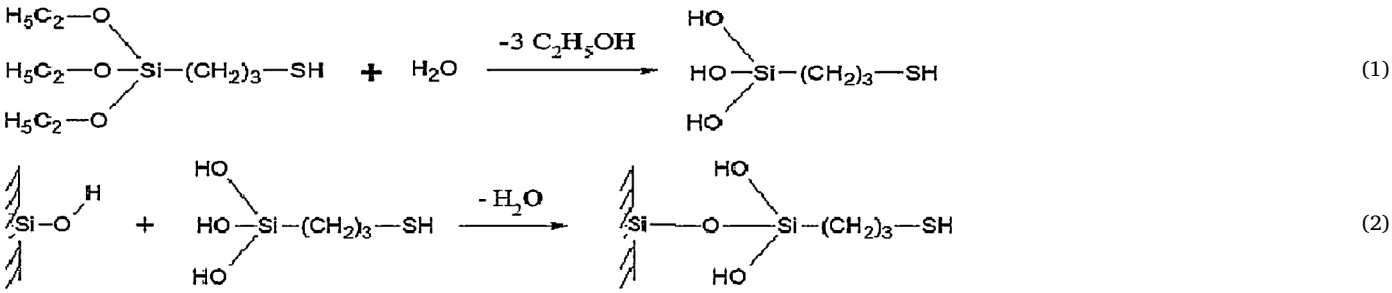

(1)

(2)

[19]. After grafting montmorillonite with 3 aminopropyltriethoxysilane, a recent study discovered a blocking phenomenon in the basal distance value d_{001} [20]. This phenomenon is thought to be caused by the simultaneous condensation of silane molecules with two adjacent montmorillonite layers. To this end, this study aims to graft Maghnite with (3 Mercaptopropyl) triethoxysilane and investigate its effect on blocking the interlamellar distance.

The objective of the present study is to master the grafting methodology of a coupling agent, such as MPTES, which results in the stabilization of the d001 value while immobilizing the alkoxysilane molecule between the layers of Maghnite. The synthesized product has potential applications as an environmental material, such as in water purification. This type of material could be integrated into filtration systems to effectively eliminate undesirable organic or inorganic substances.

2. Experimental

2.1. Materials and methods

Purified clay (Maghnite) with a CEC of 115 meq/100 g was used as the base sample in this study. Grafting was done with a trifunctional silane (3-mercaptopropyl)triethoxysilane (MPTES), an Aldrich product (≥80 %), and it was used exactly as received. Trimethyltetradecylammonium Chloride (TMTDAC), an Aldrich product with a purity of 98 %, was used as a surfactant.

2.2. Raw clay purification

The raw clay was washed with hydrogen peroxide to remove any organic matter before being dried in an oven at 80 °C for 24 h. The purified clay was ground in a mortar to achieve uniform particle sizes. Mt, the purified sample, was characterized using FRX, DRX, FTIR and TGA elemental analysis.

2.3. MPTES grafting on Mt

This was achieved by grafting an MPTES-type monomer onto the silanol groups of Mt. The chemical formula of (3-mercaptopropyl) triethoxysilane (MPTES) is as follows:

A total of 10 g of Mt were first dispersed in 200 ml of a 25/75 water/ethanol solution. Then, 8*g* of MPTES was added to the Mt suspension for 12 h at 100 °C while stirring. The grafted montmorillonite was recovered by centrifugation (4000 rpm for 30 min) and washed with dichloroethane to remove excess ungrafted silane. The Mt-MPTES product was dried in an oven (80 °C for 24 h) and analyzed using XRF, CHN (C determination), XRD, FTIR and TGA.

2.4. Modification of Mt and Mt-MPTES by TMTDAC at different CECs

This modification was carried out on Mt and Mt-MPTES as follows: a desired amount of TMTDAC was dissolved in 30 ml of distilled water, and 2*g* of Mt. 2*g* of Mt-MPTES was added to a similar suspension. The two reaction mixtures were stirred for 6 h at 60 °C in a water bath. The products obtained were washed with distilled water, recovered by centrifugation (4000 rpm^{-1}, 30 min) and dried in an oven (80 °C, 24 h). The TMTDAC concentrations used were 0.5 CEC, 1.0 CEC and 1.5 CEC. (0.5 CEC meant that the amount of TMTDAC added was 0.5 times the CEC of the Mt in the suspension). The products of modification on Mt are recovered and noted respectively: Mt-$TMTDAC_{(0.5CEC)}$, Mt-$TMTDAC_{(1.0CEC)}$ and Mt-$TMTDAC_{(1.5CEC)}$. For grafted Mt, the products recovered are, respectively: Mt-G-$TMTDAC_{(0.5CEC)}$, Mt-G-$TMTDAC_{(1.0CEC)}$ and Mt-G-$TMTDAC_{(1.5CEC)}$. The analyses performed on these samples are XRF, CHN (C and N determination), DRX, FTIR and TGA.

This modification was performed on Mt and Mt-MPTES by dissolving the desired amount of TMTDAC in 30 ml of distilled water and 2 g of Mt. Then, 2 g of Mt-MPTES was added to a similar suspension. The two reaction mixtures were stirred for 6 h in a water bath at 60 °C. The obtained products were washed with distilled water, centrifuged (4000 rpm^{-1} for 30 min), and dried in an oven (80 °C for 24 h). TMTDAC concentrations of 0.5 CEC, 1.0 CEC, and 1.5 CEC were used. 0.5 CEC meant that the TMTDAC added was 0.5 times the CEC of the Mt in suspension. The following products of Mt modification were recovered and noted: Mt-$TMTDAC_{(0.5CEC)}$, Mt-$TMTDAC_{(1.0CEC)}$ and Mt-$TMTDAC_{(1.5CEC)}$. For grafted Mt, the products recovered were: Mt-G-$TMTDAC_{(0.5CEC)}$, Mt-G-$TMTDAC_{(1.0CEC)}$ and Mt-G-$TMTDAC_{(1.5CEC)}$. These samples were subjected to XRF, CHN (C and N determination), XRD, and FTIR analyses.

2.5. Modification of Mt and Mt-MPTES by TMTDAC at different CECs

This modification was carried out on Mt and Mt-MPTES as follows: a

desired amount of TMTDAC was dissolved in 30 ml of distilled water, and 2*g* of Mt. 2*g* of Mt-MPTES was added to a similar suspension. The two reaction mixtures were stirred for 6 h at 60 °C in a water bath. The products obtained were washed with distilled water, recovered by centrifugation (4000 rpm^{-1}, 30 min) and dried in an oven (80 °C, 24 h). The TMTDAC concentrations used were 0.5 CEC, 1.0 CEC and 1.5 CEC. (0.5 CEC meant that the amount of TMTDAC added was 0.5 times the CEC of the Mt in the suspension). The products of modification on Mt are recovered and noted respectively: Mt-TMTDAC$_{(0.5CEC)}$, Mt-TMTDAC$_{(1.0CEC)}$ and Mt-TMTDAC$_{(1.5CEC)}$. For grafted Mt, the products recovered are, respectively: Mt-G-TMTDAC$_{(0.5CEC)}$, Mt-G-TMTDAC$_{(1.0-CEC)}$ and Mt-G-TMTDAC$_{(1.5CEC)}$. The analyses performed on these samples are XRF, CHN (C and N determination), DRX, FTIR and GTA.

2.6. X-ray fluorescence analysis

Philips PW 2400 XRF Ray-X Fluorescence (XRF) spectrometry was used to determine chemical compositions. The LiB_4O_7 fusion method was used to prepare the samples.

2.7. CHN test

After combustion in a high-temperature furnace, the elements C and N were detected using an infrared and thermal conductivity cell. The equipment used is a TruSpec Micro CHN analyzer (LECO), known for its efficiency and speed; the entire analysis cycle takes around 4 min.

2.8. FTIR analysis

The preparation consisted of compressing the samples with KBr to obtain pellets (297 mg of pure, dry KBr with 3 mg of solid product). This mixture was compressed under a vacuum (8 tons/cm^2) at room temperature. FTIR spectra were recorded on a brand-name instrument (Shimadzu FTIR 830 Spectrophotometer, made in Japan) over a 4000 to 400 cm^{-1} spectral range.

2.9. XRD analysis

XRD measurements were taken with a diffractometer (Philips diffractometer X'Pert Software) on the Cu-Kα line at a wavelength of $\lambda = 1.54186$ Å. Determining the diffraction angle 2Θ allows us to calculate the basal distance d_{001} using Braag's law (Eq. (3)):

$$2d_{001}.Sin\Theta = K.\lambda. \quad (3)$$

The results were recorded in the 2Θ range (1° - 80°), with a 0.02° step size and a counting time per step of 1.05 s.

2.10. TGA analysis

The analyzes were carried out under a nitrogen flow at 10 ml/ min, for a heating rate of 10 °C/ min and a temperature interval of 30 to 800 °C, using a thermogravimetric analyzer of the SHIMADZU TGA brand-51.

Table 2
Results of elemental analysis by CHN.

Samples	Mt	Mt-TMTDAC(*)	Mt-MPTES	Mt-G-TMTDAC(*)
% C	0.05	3.12	4.02	5.06
% N	-	2.11	–	1.42

(*) The sample subjected to XRF and CHN is the 1.5 CEC sample from Mt.

3. Results and discussion

3.1. X-ray fluorescence analysis

The results of the various elemental analyses (XRF and CHN) performed on samples Mt, Mt-TMTDAC(*), Mt-MPTES, and Mt-G-TMTDAC(*) suggest a hypothesis in favor of silane grafting and modification with alkylammonium, (Table 1). A significant increase in SiO_2 and SO_3 levels from 55.22 % and 0.51 %, respectively, in Mt to 58.28 % and 3.22 % in Mt-MPTES, which includes Si and S in its chemical structure.

3.2. CHN test

The results obtained by CHN (Table 2) indicate carbon levels estimated at 0.05 %, 3.12 %, 4.02 % and 5.06 % attributed respectively to Mt, Mt-TMTDAC(*), Mt-MPTES and Mt-G-TMTDAC (*) and nitrogen levels estimated at 2.11 % and 1.42 % respectively for Mt-TMTDAC(*) and Mt-G-TMTDAC(*). These results highlight the presence of carbon (surfactant alkyl chains and silane alkoxy groups) and nitrogen (surfactant NH_3^+ ammonium groups). The 1.42 % nitrogen content of Mt-G-TMTDAC(*) is lower than the 2.11 % of Mt-TMTDAC(*). Moreover, grafted silane molecules condensing between the Mt sheets leave little space for the TMTDAC alkyl chains, in contrast to the ungrafted Mt.

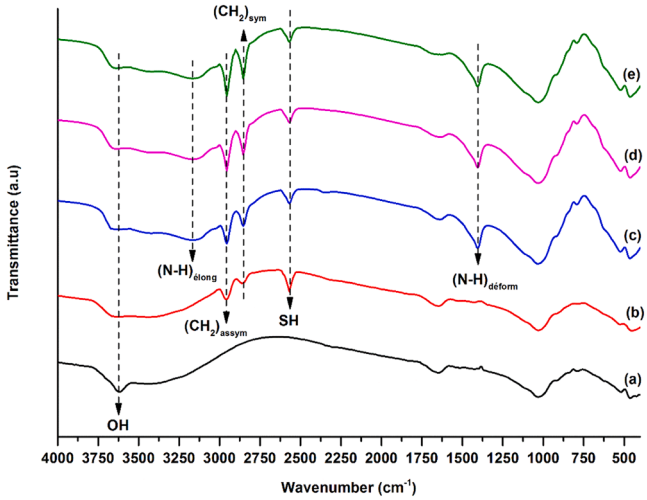

Fig. 1. FTIR spectra of: (a) Mt, (b) Mt-MPTES, (c) Mt-G-TMTDAC$_{(0.5CEC)}$, (d) Mt-G-TMTDAC$_{(1.0CEC)}$ and (e) Mt-G-TMTDAC$_{(1.5CEC)}$.

Table 1
XRF elemental analysis results.

Content (%)	SiO_2	Al_2O_3	Fe_2O_3	CaO	MgO	SO_3	K_2O	Na_2O
Mt	**55.22**	18.04	3.32	1.35	4.93	**0.51**	1.19	1.88
Mt-TMTDAC (*)	55.18	18.10	2.22	0.79	3.65	0.50	1.01	1.66
Mt-MPTES	**58.28**	18.20	2.14	0.60	3.10	**3.22**	0.78	1.75
Mt-G-TMTDAC (*)	58.20	17.99	2.15	0.08	2.32	3.20	0.66	1.42

3.3. FTIR analysis

Fig. 1 shows the FTIR spectra of five samples: Mt (a), Mt-MPTES (b), Mt-G-TMTDAC$_{(0.5CEC)}$ (c), Mt-G-TMTDAC$_{(1.0CEC)}$ (d) and Mt-G-TMTDAC$_{(1.5CEC)}$ (e). In spectrum (b), it can be noted that the majority of the bands in the spectrum (a) were retained, but new bands at 2954.7 cm^{-1}, 2854.4 $cm^{-1,}$ and 2569 cm^{-1} appeared, attributed respectively to the asymmetric and symmetric stretching vibrations -CH_2 of the alkyl chain [21] and the thiol (SH) function of the silane molecules [22]. LeAnna Survant et al. highlighted the presence of the absorption band corresponding to the thiol (SH) functional group at 2548 cm^{-1} following the grafting of a silane bearing this functional group [22]. This finding confirms the grafting of MPTES onto the surface of the Mt sheets. The decrease in intensity of the band located at 3624 cm^{-1} (attributed to OH of silanols and aluminons located at the tetrahedral and octahedral layers edges) in the Mt-MPTES sample compared to that of the Mt can be explained by the reaction of the silanols of the tetrahedra with the silanols of the hydrolyzed silane molecules forming a Si-O-Si siloxane bridge. It was followed by the condensation of the silanols with each other forming a Si-O-Si-based network with the two adjacent layers during the grafting process (Fig. 5). Spectra (c), (d) and (e) in Fig. 1 for Mt-G-TMTDAC at 0.5CEC, 1.0CEC and 1.5CEC, respectively, also show bands at 2954.7 cm^{-1}, 2854.4 cm^{-1} attributed to the asymmetric and symmetric -CH_2. However, the intensity of these two bands increased after each TMTDAC modification due to the increase in TMTDAC concentration. Ismail Ltifi et al. also demonstrated that the intensity of the absorption bands at 2936 cm^{-1} and 2871 cm^{-1}, attributed to CH_2 *asym* and CH_2 *sym* respectively, increases with the CEC [23]. Bands at 3163 cm^{-1} and 1404 cm^{-1} can be attributed to N—H elongation vibration and N—H surfactant deformation, respectively [24].

3.4. XRD analysis

The basal distance d_{001} of Mt was 14.22 Å (Fig. 2a). After grafting, its value increased to 21.47 Å

(Fig. 3a), as shown in Fig. 4, Wentao He et al. confirmed the grafting of a silane onto montmorillonite through the increase in d_{001} [25], confirming the insertion of MPTES between the Mt galleries [26,27]. This value remained unchanged after further modification reactions on Mt-MPTES by TMTDAC at different CECs (Fig. 3b, 3c and 3d), while this distance increased to 27.58 Å when modifications by TMTDAC were made on ungrafted Mt (Fig. 2b, 2c and 2d), as detailed by Fig. 5. Ismail Ltifi et al. demonstrated in a study on the modification of clay with alkylammonium that the interlayer spacing increases with the CEC of the surfactant [23]. This result confirms that the MPTES grafted onto the surfaces of the Mt interlayers. Moreover, the morphology and structure of the grafted Mt were preserved despite the surfactant intercalation process. We can deduce that the binding effect of d_{001} occurred during grafting due to the condensation of silane molecules with the two adjacent Mt layers. The deposited silane molecules were hydrolyzed to silanols by the water between the Mt layers, leading to the condensation of these silanols, which probably formed oligomers with the adjacent Mt layers [28]. The latter acted as pillars, fixing the value of d_{001}, thus blocking the space between two adjacent Mt layers.

3.5. TGA analysis

The aim of the TGA tests is to prove that the grafting reactions with silane and the intercalations with alkylammonium have indeed taken place, evidenced by the increase in the hydrophobic character of each sample due to the presence of a polar organic groups between the layers of the magnetite. The Mt thermogram (Fig. 6) reveals two stages of degradation. The first mass loss, located in the temperature range of 30 – 200 °C, is estimated at 9.05 % and is attributed to the desorption of physisorbed water and the dehydration of interlamellar cations. The second temperature range (600 – 750 °C) shows a mass loss estimated at 2.31 %, attributed to the deshydroxylation of the aluminosilicates in the sheets (Table 3) [29].

The thermogram of Mt-MPTES (Fig. 6) shows three stages of degradation: the first at (30–200 °C), the second at (200–600 °C), and the final one at (600–750 °C), estimated at (6.65 %), (45.60 %), and (2.80 %) respectively. The 6.65 % mass loss observed in the first temperature range is lower than the 9.05 % indicated for Mt in the same temperature range. This decrease is explained by the hydrophobic nature of Mt-MPTES, due to the presence of organic (propyl) chains in the silane between the montmorillonite layers. The second stage of degradation (200–600 °C), evaluated at 45.60 %, corresponds to the decomposition temperature range of the grafted silane on the silicate layer [12]. The final stage of degradation (600–750 °C) shows a mass loss of 2.80 %, attributed to the dehydroxylation of the aluminosilicate sheets (Table 3).

According to Fig. 6, the thermogram of Mt-G-TMTDAC $_{(1.5\ CEC)}$ shows three stages of degradation: the first at 30–200 °C, the second at 200–600 °C, and the third at 600–750 °C, with mass losses estimated at 2.60 %, 63.30 %, and 4.13 %, respectively. The 2.60 % mass loss observed in the first stage is lower than the 6.65 % indicated for Mt-MPTES. This decrease is due to an increase in the hydrophobic nature

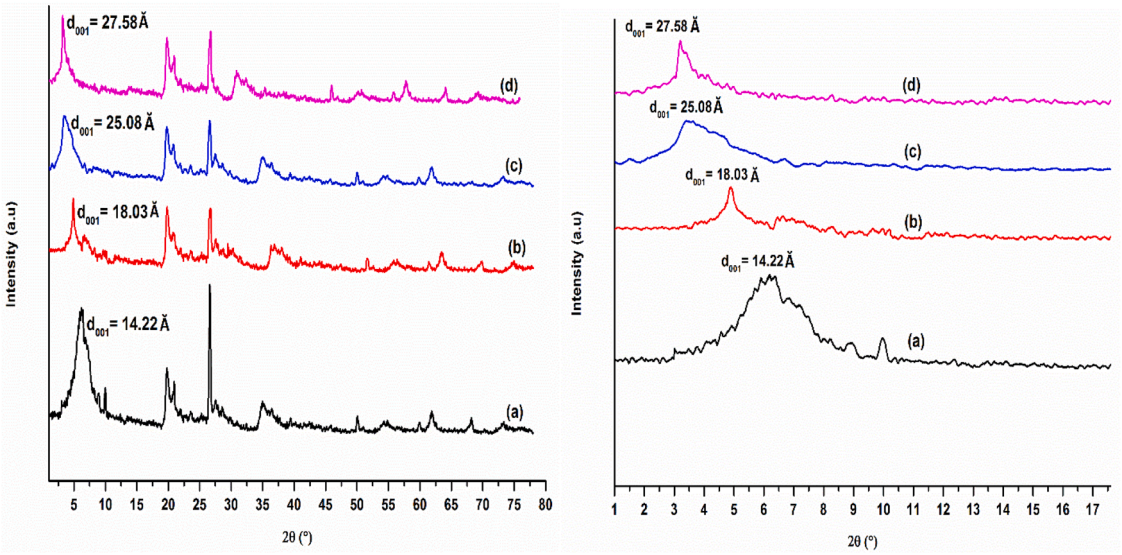

Fig. 2. (a) Diffractograms of Mt, (b) Mt-TMTDAC$_{(0.5CEC)}$, (c) Mt-TMTDAC$_{(1.0CEC)}$ (d) Mt-TMTDAC$_{(1.5CEC)}$.

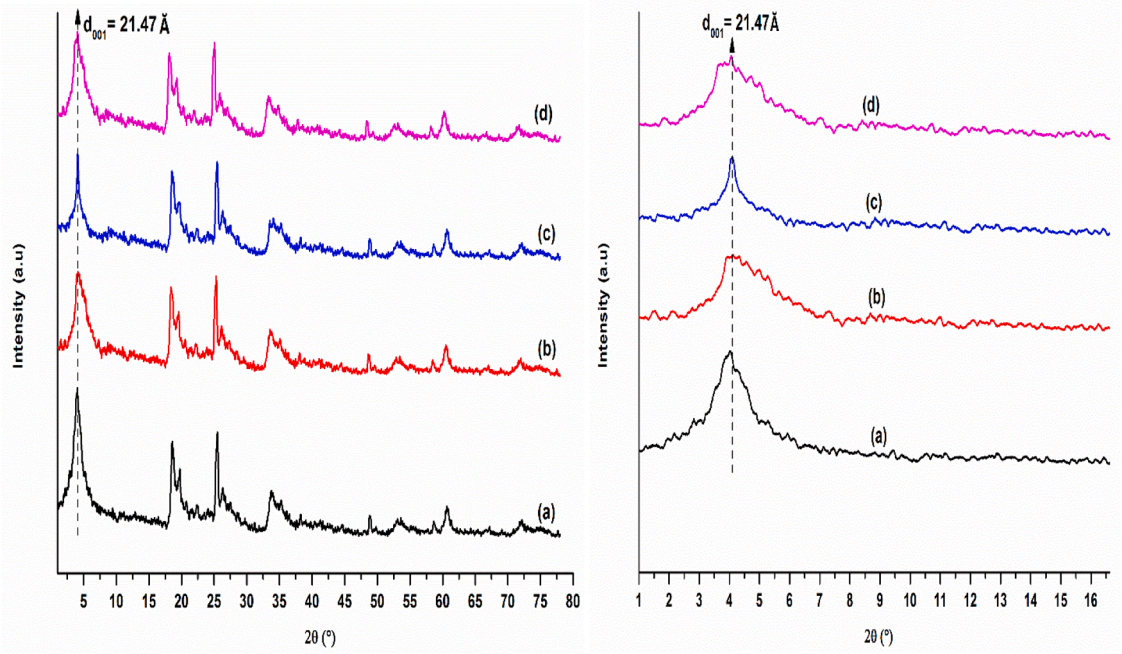

Fig. 3. Diffractograms of: (a) Mt-MPTES, (b) Mt-G-TMTDAC$_{(0.5CEC)}$, (c) Mt-G-TMTDAC$_{(1.0CEC)}$, (d) Mt-G-TMTDAC$_{(1.5CEC)}$.

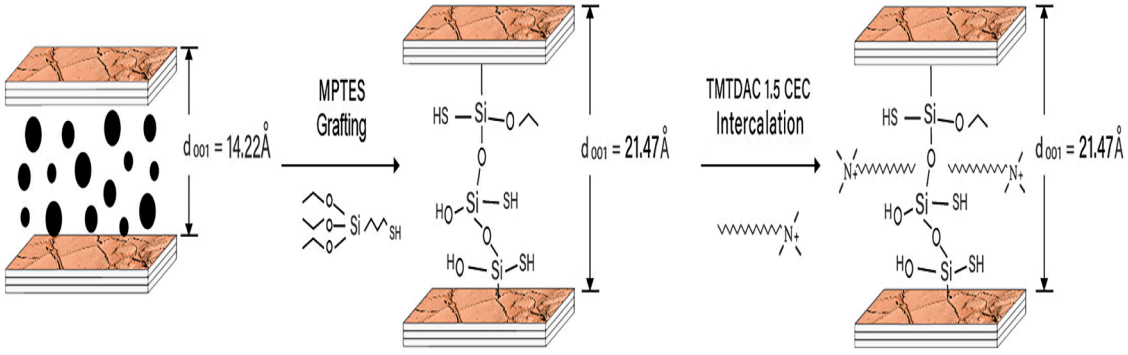

Fig. 4. Schematic illustration of MPTES grafting of Mt followed by intercalation using TMTDAC$_{(1.5CEC)}$ as an example.

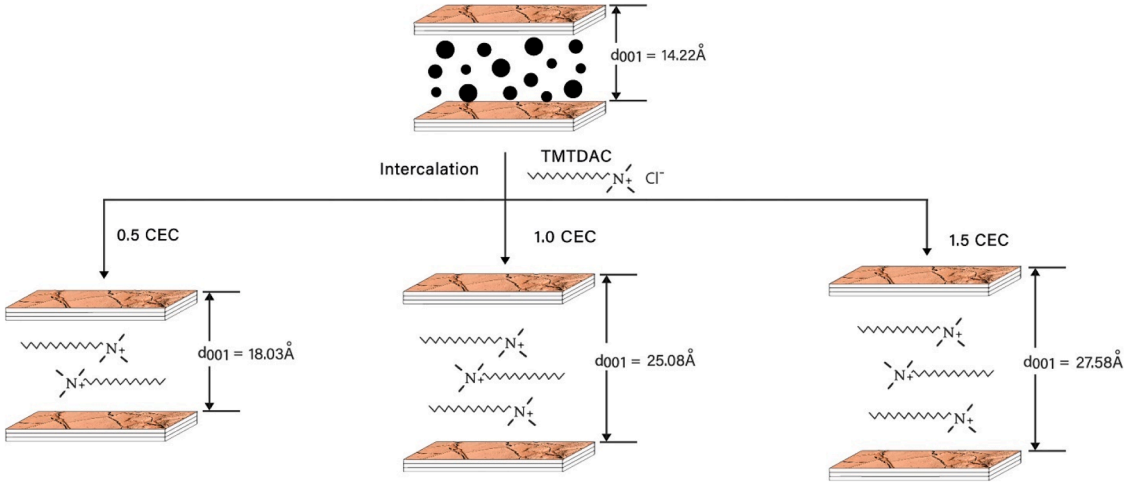

Fig. 5. Schematic illustration of TMTDAC intercalation of Mt at different CECs.

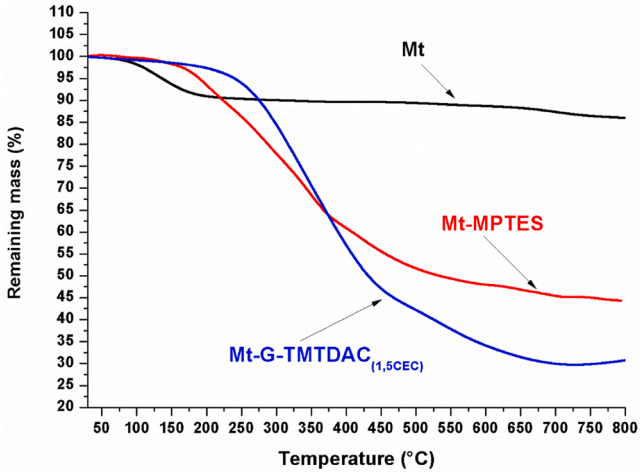

Fig. 6. Thermograms of: Mt, Mt-MPTES, and Mt-G-TMTDAC $_{(51.5\ CEC)}$.

Table 3
Results of TGA: Mt TGA, Mt-MPTES and Mt-G-TMTDAC$_{(1.5CEC)}$.

	Mt	Mt-MPTES	Mt-G-TMTDAC$_{(1.5CEC)}$
1st variation	30 – 200 °C	30 – 200 °C	30 – 200 °C
Mass loss (%)	**9.05**	**6.65**	**2.60**
2nd variation	–	200 – 600 °C	200 – 600 °C
Mass loss (%)	–	**45.60**	**63.30**
3rd variation	600 – 750 °C	600 – 750 °C	600 – 750 °C
Mass loss (%)	**2.31**	**2.80**	**4.13**
Total as a % of physisorbed and chemisorbed water content	**11.36**	**9.40**	**6.73**

of the material, caused by the presence of apolar alkyl chains of TMTDAC in the interlamellar space of Maghnite. The second stage, with an estimated 63.30 % mass loss, is mainly attributed to the degradation of alkylammonium and silane. The interval 600–750 °C displays a mass loss of 4.13 %, attributed to the dehydroxylation of the aluminosilicate sheets. Table 3 presents the total water loss percentage for the three types of samples: Mt = 11.36 %, Mt-MPTES = 9.40 %, and Mt-G-TMTDAC (1.5 CEC) = 6.73 %. This indicates that the hydrophobicity increases in the order: Mt < Mt-MPTES < Mt-G-TMTDAC (1.5 CEC), confirming the success of the grafting and intercalation reactions.

4. Conclusion

In this study, the interlayer surfaces of Maghnite were successfully grafted with MPTES. This finding is supported by the appearance on the FTIR spectrum of the thiol function (SH) band at 2569 cm^{-1} and the -CH_2 bands at 2954 cm^{-1} and 2854 cm^{-1}. The condensation of hydrolyzed silane molecules and existing silanol groups at the surfaces of adjacent Maghnite layers formed a bridge, which fixed the basal distance value of Mt-MPTES at 21.47 Å despite TMTDAC intercalation at various concentrations. This phenomenon could lead to the developing of a new material with reactive organic group immobilization and controlled swelling properties.

The three ATG analyses showed a reduction in water loss rates each time the Maghnite was subjected to grafting and intercalation. These processes respectively enhance the hydrophobic character, which can be explained by the presence of silane and alkylammonium between the clay layers, thus confirming the success of these reactions. A grafted montmorillonite with a silane, featuring a blocked basal spacing (d_{001}), offers unique possibilities due to its enhanced properties, such as its use as a water purifier. The functional groups introduced by the grafted silane can specifically interact with pollutants, such as heavy metals (lead, mercury), by forming chemical complexes. Organic substances (such as pesticides or pharmaceuticals) can be trapped through hydrophobic interactions or specific bonding. The blocked basal spacing ensures good accessibility of pollutants to the internal surface, allowing for a high and sustained adsorption capacity. This blocking can also prevent the loss of intercalated substances, ensuring long-term efficiency. The chemical modifications introduced by the silane can be tailored to target specific pollutants (for example, by grafting acidic groups to capture metal cations or amine groups for anions).

CRediT authorship contribution statement

Deghfel Nadir: Methodology, Conceptualization. **Melouki Azzedine:** Writing – original draft, Validation, Resources, Formal analysis. **Benyahia Azzedine:** Formal analysis, Data curation. **Farsi Chouki:** Supervision. **Laib Nouri:** Funding acquisition. **Khodja Mohammed Abdallah:** Validation.

Declaration of competing interest

The authors declare that they have no known competing financial interests or personal relationships that could have appeared to influence the work reported in this paper.

Acknowledgments

The authors would like to thank Prof. Dr. Azzedine BENYAHIA for his scientific and technical support throughout the preparation of this work.

Data availability

The data that has been used is confidential.

References

[1] Q. Zhao, H. Choo, A. Bhatt, S.E. Burns, B. Bate, Review of the fundamental geochemical and physical behaviors of organoclays in barrier applications, Appl. Clay. Sci. 142 (2017) 2–20. https://doi:10.1016/j.clay.2016.11.024.
[2] Q.D. Dao, N.E. Gorji, A. Alhodaib, et al., Fabrication, characterization and simulation analysis of perovskite solar cells with dopant-free solution-processible C_6PCH_2 hole transporting material, Opt. Quant. Electr. 54 (2022) 278, https://doi.org/10.1007/s11082-022-03638-3.
[3] A. Melouki, S. Terchi, D. Ouali, A. Bounab, Preparation of new copolymer (polystyrene/TMSPM grafted on DDA-fractionated algerian montmorillonite) hybrid organoclay by radical copolymerization: structural study, thermal stability and hydrophobicity area, J. Therm. Anal. Cal. 147 (2021) 5637–5648. https://doi:10.1007/s10973-021-10935-8.
[4] S. Hu, Y. Liu, L. Wei, D. Luo, Q. Wu, X. Huang, T. Xiao, Recent advances in clay minerals for groundwater pollution control and remediation, Environ. Sci. Pollution Res. 31 (17) (2024) 24724–24744, https://doi.org/10.1007/s11356-024-32911-z.
[5] I.K. Tonle, E. Ngameni, D. Njopwouo, C. Carteret, A. Walcarius, Functionalization of natural smectite-type clays by grafting with organosilanes: physico-chemical characterization and application to mercury (II) uptake, Phys. Chem. Chem. Phys. 5 (2003) 4951–4961. https://doi:10.1039/B308787E.
[6] W. Xiang, S. Qiang, H. Yumei, et al., Structure and thermal stability of PMMA/MMT nanocomposites as denture base material, J. Therm. Anal. Calorim. 115 (2014) 1143–1151. https://doi:10.1007/s10973-013-3412-9.
[7] Y. Long, X. Zhisheng, Z. Jun, Influence of nanoparticle geometry on the thermal stability and flame retardancy of high-impact polystyrene nanocomposites, J. Therm. Anal. Calorim. 130 (2017) 1987–1996, https://doi.org/10.1007/s10973-017-6514-y.
[8] M.D.R. Perera, R.A.L.R. Amarasena, W.M.A.T. Bandara, R. Weerasooriya, L. Jayarathna, Surfactant-modified clay composites: water treatment applications. Clay Composites: Environmental Applications, Springer Nature Singapore, Singapore, 2023, pp. 233–252, https://doi.org/10.1007/978-981-99-2544-5_11.
[9] H. Wang, D. Zhang, Y. Zhao, M. Xie, Colloids and Surfaces A: physicochemical and engineering aspects cationic surfactant modified attapulgite for removal of phenol from wastewater, Colloids Surf. A Physicochem. Eng. Aspects 641 (2022) 128479, https://doi.org/10.1016/j.colsurfa.2022.128479.
[10] M. Hiranchansook, S. Jakpet, N. Trongsiriwat, L. Simasatitkul, S. Pranee, S. Seeyangnok, Enhancing oil absorption capacity through innovative bentonite

modification with cationic surfactants, South Afr. J. Chem. 78 (1) (2024) 293–299, https://doi.org/10.17159/0379-4350/2024/v78a37.
[11] M. Tuchowska, B. Muir, M. Kowalik, et al., Sorption of molybdates and tungstates on functionalized montmorillonites: structural and textural features, Materials (Basel) 12 (2019) 2253. https://doi:10.3390/ma12142253.
[12] N.N. Herrera, J.M. Letoffe, J.L. Putaux, et al., Aqueous dispersions of silane functionalized laponite clay platelets. A first step toward the elaboration of water-based polymer/clay nanocomposites, Langmuir 20 (2004) 1564–1571, https://doi.org/10.1021/la0349267.
[13] Z.P. Tomić, L. Kaluđerović, N. Nikolić, S. Marković, P. Makreski, Thermal investigation of acetochlor adsorption on inorganic and organic modified montmorillonite, J. Thermal. Anal. Calorim. 123 (2016) 2313–2319. https://doi:10.1007/s10973-015-5102-2.
[14] Z.H. Zhang, T.S. Li, F. Yang, et al., Montmorillonite clay catalysis XI1: protection and deprotection of hydroxyl group by formation and cleavage of trimethylsilyl ethers catalysed by Montmorillonite K-10, Synth. Commun 28 (1998) 3105–3114, https://doi.org/10.1080/00397919808004891.
[15] M. Ogawa, S. Okutomo, K. Kuroda, Control of interlayer microstructures of a layered silicate by surface modified cation with organochlorosilanes, J. Am. Chem. Soc. 120 (1998) 7361–7362, https://doi.org/10.1021/ja981055s.
[16] M. Asgari, U. Sundararaj, Silane functionalization of sodium montmorillonite nanoclay: the effect of dispersing media on intercalation and chemical grafting, Appl. Clay Sci. 153 (2018) 228–238. https://doi:10.1016/j.clay.2017.12.020.
[17] P.T. Bertuoli, D. Piazza, L.C. Scienza, A.J. Zattera, Preparation and characterization of montmorillonite modified with 3-aminopropyltriethoxysilane, Appl. Clay Sci. 87 (2014) 46–51. https://doi10.1016/j.clay.2013.11.020.
[18] M. Park, I.K. Shim, E.Y. Jung, J.H. Choy, Modification of external surface of laponite by silane grafting, J. Phys. Chem. Solids. 65 (2004) 499–501, https://doi.org/10.1016/j.jpcs.2003.10.031.
[19] S. Wei, H. Hong Ping, Z.Jian Xi, Y. Peng, M.A. Yue Hong, L. XiaoLiang, Preparation and characterization of 3-aminopropyltriethoxysilane grafted montmorillonite and acid-activated montmorillonite, Chinese Sci. Bull. 54 (2009) 265–271, https://doi.org/10.1007/s11434-008-0361-y.
[20] Su. Linna, Qi. Tao, He. Hongping, Zhu. Jianxi, Locking effect: a novel insight in the silylation of montmorillonite surfacesMater, Chem. Phys. 136 (2012) 292–295. https://doi:10.1016/j.matchemphys.2012.07.010.
[21] N. Ladjal, B. Zidelkheir, S. Terchi, Influence of actadecylammonium, N, N dimethylhexadecylammonium and 1-hexadecyltrimethylammonium chloride upon the fractionated montmorillonite, J. Therm. Anal. Cal 134 (2018) 1–8. https://doi:10.1007/s10973-018-7237-4.
[22] L. Survant, M. Andrejevic, J. Picker, Surface-initiated polymerization of styrene from one-step prepared thiol-functionalized organoclays, Polyhedron 41 (2016) 114 37. https://doi10.1016/j.poly.2015.09.027.
[23] Ismail Ltifi, Fadhila Ayari, Dalila Ben Hassen Chehimi, et al., Physicochemical characteristics of organophilic clays prepared using two organo-modifiers : alkylammonium cation arrangement models, Appl. Wter Sci. 8 (2018) 91, https://doi.org/10.1007/s13201-018-0732-8.
[24] P. Aranda, E. Ruiz-Hitzky, Poly (ethylene oxide)/NH_4^+smectite nanocomposites, Appl. Clay Sci. 15 (1999) 119–135. https://qmro.qmul.ac.uk/xmlui/bitstream/123456789/1854/1/CHENPolymerClay2004.pdf.
[25] H. Wentao, Y. Yong, H. Min et al. Influence of reaction conditions on the grafting pattern of 3 glycidoxypropyl trimethoxysilane on Montmorillonite. Bull. Korean Chem. Soc. 34 (2013) 112.
[26] K. Isoda, K. Kuroda, M. OgawaInterlamellar, Grafting of γ-methacryloxypropylsilyl groups on magadiite and copolymerization with methyl methacrylate, Chem. Mater 12 (2000) 1702–1707.
[27] K.W. Park, S.Y. Jeong, O.Y. Kwon, Interlamellar silylation of H-kenyaite with 3-aminopropyltriethoxysilane, Appl. Clay Sci. 27 (2004) 21–27. https://doi:10.1016/j.clay.2003.12.003.
[28] A. Melouki, S. Terchi, D. Ouali, Grafting of 3 mercaptopropyl triethoxysilane onto dodecylamuonium intercaled Algerian montmorillonite; characterizations and application for synthesis of polystyrene/organoclay hybrid material by radical polymerization, J. New Technol. Mater. 11 (2021) 10–18. https://doi:10.12816/0060294.
[29] A. Elkhalifah, S. Maitra, M.A. Bustam, T. Murugesan, J. Therm. Anal. Calorim. 110 (2012) 765–771.